

Trapping of interacting propelled colloidal particles in inhomogeneous media

Martin P. Magiera and Lothar Brendel

Faculty of Physics and CENIDE, University of Duisburg-Essen, D-47048 Duisburg, Germany

(Dated: August 30, 2018)

A trapping mechanism for propelled colloidal particles based on an inhomogeneous drive is presented and studied by means of computer simulations. In experiments this method can be realized using photophoretic Janus particles driven by a light source, which shines through a shading mask and leads to an accumulation of the particles in the passive part. An equation for an accumulation parameter is derived using the effective inhomogeneous diffusion constant generated by the inhomogeneous drive. The impact of particle interaction on the trapping mechanism is studied, as well as the interplay between passivity-induced trapping and the emergent self-clustering of systems containing a high density of active particles. The combination of both effects makes the clusters more controllable for applications.

PACS numbers: 82.70.Dd, 05.40.Jc, 05.70.Ln, 47.57.-s

I. INTRODUCTION

In recent years, various approaches have been pursued to construct propelled colloidal particles, including man-made active swimmers at the micron scale. Such objects undergo Brownian motion driven by equilibrium thermal fluctuations, but are also driven by a propulsion mechanism out of equilibrium, resulting in an interplay between equilibrium thermal motion and non-equilibrium drive [1, 2]. Besides the construction of artificial flagella [3] which mimic natural microswimmers like bacteria, algae or sperm or the use of molecular machines [4], novel nano motors have been proposed to drive passive colloids. An elegant way to bring passive colloids into motion is the generation of chemical, electrostatic or thermal field gradients [5, 6] leading to a net propulsion via chemophoresis, electrophoresis or thermophoresis. Introducing an inhomogeneous coating of the colloidal particle leads to a self-generated slip velocity pattern at the colloidal surface [7], inducing a net propulsion of particles via self-thermophoresis [8, 9] or self-diffusiophoresis [10–14]. For the case of thermophoresis, the inhomogeneous absorption of light causes inhomogeneous heating of the particle, which again leads to a temperature gradient in the medium and to propulsion, called photophoresis. While most diffusiophoretic swimmers based on catalytic reactions require a fuel in the liquid (typically hydrogen peroxide; a fuel free exception is e.g. a swimmer in a binary mixture near the critical demixing temperature used in Refs. [13, 14]), swimmers based on photophoresis are fuel free, which makes them suitable for in-vivo applications.

The control of objects in liquids is of fundamental interest. Instead of passive colloids, propelled colloidal particles move autonomously in the liquid where they can fulfill a task, e.g., a catalytic reaction taking place at the swimmer surface in a lab-on-the-chip device or in nature to cure an ecosystem (bioremediation). External control like steering, trapping or sorting of active matter can facilitate the swimmers' remove from the system after the task is fulfilled. One realization is the introduction of a geometrical trap as proposed in Ref. [15] (or

Ref. [16] for chiral swimmers) which collects all active particles after the task is fulfilled. In recent experiments, passive nano-objects have been trapped thermophoretically in an inhomogeneous temperature field generated by gold patterns illuminated by a focused laser beam [17]. In another work, active photophoretic swimmers have been trapped using a complex feedback control mechanism [18]. Therefore, the orientation of individual swimmer has been recorded. According to the orientation, swimmers are accelerated when they aim at a predefined target.

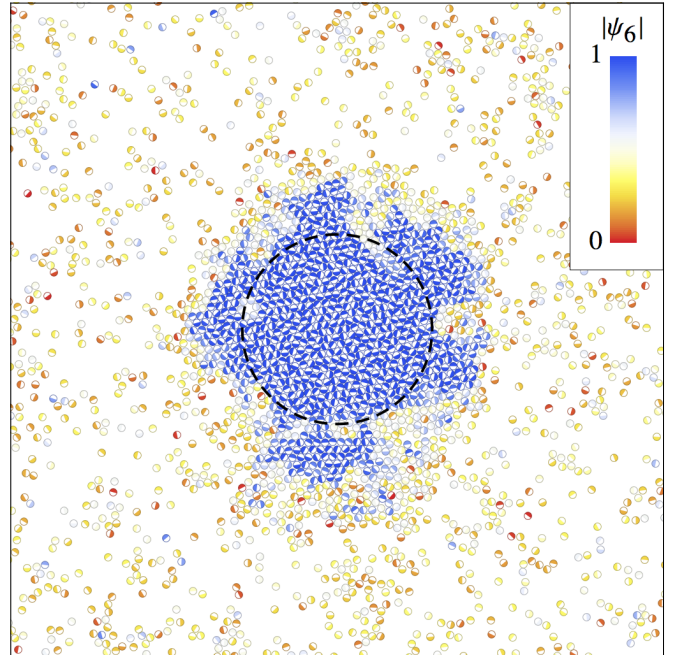


FIG. 1. Snapshot of a simulation for a system of interacting active particles (at $Pe=250$ and a particle density of $\phi_p=0.25$ defined in Eq (15)), which are passivated in a spherical region and accumulate there. The color coding shows the bond order parameter, which is introduced in Eq. (18) and quantifies local crystallization of particles.

Using theory and computer simulations, we study the trapping of particles by only manipulating the propulsion mechanism (or in a biological way by manipulating their tumbling rate) without any feedback control mechanism. Whenever swimming objects interact with each other, their dynamics is influenced by the interaction. Recently, it has been shown that system which interact only via repulsive interactions can accumulate driven by activity when driving and density are large enough. This *athermal phase separation* [19–23] is related to our study as it is based on inhomogeneities of, e.g., the diffusion constant in regions, where spontaneously a higher particle density exists. However, in solely active systems, these inhomogeneities are generated dynamically and cannot be controlled externally. Turning off the propulsion in a part of the system leads to an accumulation of particles, a fact which is known [24–26] and observed in experiments [27] but has not been addressed explicitly in an own publication to the knowledge of the authors. We show that the local *marking* of the target region can be used to induce the emergent athermal phase separation, which enhances the effect of accumulation.

II. MODEL

We describe Janus particles suspended in a viscous liquid using Brownian Dynamics, which is Langevin dynamics in the overdamped limit. This limit is essential in the low Reynolds number limit [28, 29]. It is governed by the equations for position and orientation of particle i :

$$\dot{\mathbf{r}}_i = \sqrt{2D}\boldsymbol{\eta}_i(t) + \mathbf{F}_i/\gamma \quad (1a)$$

$$\boldsymbol{\omega}_i = \sqrt{2D_r}\boldsymbol{\eta}_i^r(t) + \mathbf{T}_i/\gamma_r \quad (1b)$$

$$\dot{\hat{\mathbf{o}}}_i = \boldsymbol{\omega}_i \times \hat{\mathbf{o}}_i, \quad (1c)$$

with \mathbf{F}_i and \mathbf{T}_i representing all forces and torques acting at particle i , the latter being neglected in this work. The vectors $\boldsymbol{\eta}_i(t)$ and $\boldsymbol{\eta}_i^r(t)$ contain uncorrelated, normally distributed noise with zero mean and second moment 1 [30], which is motivated by a strict separation of the timescales of the particle friction due to particle liquid collisions and particle motion. The spatial diffusion coefficient D depends on temperature and Stokes' damping γ via $D=\gamma/(k_B T)$. For the rotational diffusion coefficient (spherical particles) the particle diameter σ enters via $D_r = 3D/\sigma^2 = \gamma_r/(k_B T)$ if we assume no slip between a particles' surface and the liquid [31]. The equations of motion can be solved using Euler's or higher order methods.

Having introduced a model for spherical particles suspended in a solvent, we now introduce a propulsion via a self-propulsion velocity v_{sp} in terms of an effective force, as well as interactions via a pair potential Φ ,

$$\mathbf{F}_i = \gamma v_{sp}(\mathbf{r}_i)\hat{\mathbf{o}}_i - \sum_j \nabla_i \Phi(\mathbf{r}_i - \mathbf{r}_j). \quad (2)$$

Thus, the self-propulsion velocity points into the direction of a particle's orientation $\hat{\mathbf{o}}_i$ and depends on the particle's position \mathbf{r}_i . The two motion mechanisms, passive thermal diffusion and active motion due to propulsion, are compared in the dimensionless Péclet number

$$Pe = \frac{\sigma v_{sp}}{D}, \quad (3)$$

which is of fundamental importance in this work.

As a pair potential we use the truncated Lennard-Jones potential [32],

$$\Phi(\mathbf{r}) = \begin{cases} 4\epsilon \left(\left(\frac{\sigma}{r}\right)^{12} - \left(\frac{\sigma}{r}\right)^6 \right) + \epsilon & r \leq 2^{1/6}\sigma \\ 0 & r > 2^{1/6}\sigma \end{cases}, \quad (4)$$

which contains only the repulsive core of the common Lennard-Jones potential. For the interaction energy we choose either $\epsilon=100k_B T$ or zero for the case of no interaction. In regions of large particle densities, particles can crystallize with a lattice constant starting of $2^{1/6}\sigma$ at intermediate density and slightly decreasing with rising density. Note that when disregarding rotational Brownian motion, actually the particles do not have a physical *extension*, but only define a length caused by interaction.

III. SYSTEM GEOMETRY

We study a system with two regions: In the active one, \mathcal{A} , objects are propelled ($v_{sp}(\mathbf{r}) = v_{sp}^0 > 0$) while in the other, \mathcal{P} , only thermal diffusion takes place since $v_{sp}(\mathbf{r}) = 0$. Because this is the only inhomogeneity type of $v_{sp}(\mathbf{r})$ considered and for the sake of brevity, we denote in the following the constant v_{sp}^0 by v_{sp} as well. The corresponding propulsion of particles in the illuminated region prevents the system to reach equilibrium: In the non-equilibrium steady state, particles accumulate in the passive region, as shown in Fig. 1.

To quantify the accumulation, it is convenient to evaluate the difference between the densities in the passive region \mathcal{P} and the active region \mathcal{A} , which are defined by

$$\rho_{\mathcal{P}} = \frac{N_{\mathcal{P}}}{V_{\mathcal{P}}} \quad \text{and} \quad \rho_{\mathcal{A}} = \frac{N - N_{\mathcal{P}}}{V - V_{\mathcal{P}}}, \quad (5)$$

where N and V are the total number of particles and total volume of the system, respectively. For the case that all particles are captured in region \mathcal{P} , the density difference becomes $N/V_{\mathcal{P}}$. We use this maximum value to normalize the density difference, and define the accumulation parameter

$$\Delta = \frac{\rho_{\mathcal{P}} - \rho_{\mathcal{A}}}{N/V_{\mathcal{P}}} = \frac{\frac{N_{\mathcal{P}}}{N} - \frac{V_{\mathcal{P}}}{V}}{1 - \frac{V_{\mathcal{P}}}{V}}. \quad (6)$$

Now, this parameter is unity for the case that all particles are trapped in the passivation volume of relative size $\phi=V_{\mathcal{P}}/V$ while it is zero for a homogeneous swimmer distribution (to be expected in the limit $T \rightarrow \infty$). In a finite

system, it can even become negative due to fluctuations. Note as well that due to the normalization, Δ vanishes in the thermodynamic limit ($V \rightarrow \infty$, V_p fixed), which we do not consider here, though.

The accumulation parameter can be also written in terms of the excess density α defined by $\rho_p = \rho_A(1 + \alpha)$ or

$$\alpha = \frac{\rho_p}{\rho_A} - 1 \quad (7)$$

$$\Delta = \frac{1}{1 + \frac{1}{\alpha\phi}}. \quad (8)$$

In the following, we will derive an expression for the accumulation parameter Δ . We assume that the particle density in the active region \mathcal{A} is homogenous. The homogenization is driven by thermal diffusion D (as it is in the passive region \mathcal{P}) as well as the combination of random rotation D_r and driving v_{sp} .

IV. ACCUMULATION

A. Low particle density: No interaction

Let us first assume the case of low particle density, where particle-particle interaction can be neglected. The relevant physics take place at the boundary between \mathcal{P} and \mathcal{A} . Particle flow due to random motion is described by Fick's first law of diffusion which usually leads to a homogeneous density profile in the steady state. Here, however, the underlying system shows an inhomogeneity: In \mathcal{A} the particles are driven and are subjected to random rotation, which introduces a *persistence length* $\ell_{p,\mathcal{A}}$ after which the previous particle orientation is forgotten. On larger scales this corresponds to Brownian motion with steps of size $\ell_{p,\mathcal{A}}$. In \mathcal{P} the step size, stemming solely from D is smaller. Hence, we get an inhomogeneous effective diffusion coefficient D_{eff} as derived below.

Taking this inhomogeneity due to a gradient in step size into account, we arrive at an extended Fick's law of diffusion [24, 25],

$$J = -D_{\text{eff}} \nabla \rho - \frac{\rho}{2} \nabla D_{\text{eff}}, \quad (9)$$

to be used in the description of a particle flow from one region to the other. In the steady state the total flux vanishes, and the particle injection through the second term is completely balanced by the usual diffusion current. The solution of this flux equation is

$$\rho \sqrt{D_{\text{eff}}} = \text{const.} \quad \Rightarrow \quad \frac{\rho_p}{\rho_A} = \sqrt{\frac{D_{\mathcal{A}}}{D_{\mathcal{P}}}} = \alpha + 1, \quad (10)$$

where ρ_i and D_i are homogeneous particle densities and effective diffusion constants in the corresponding regions.

In \mathcal{P} the effective diffusion equals the thermal D . We now restrict ourselves to a two-dimensional system of self-propelled particles [33] with a self-propulsion velocity

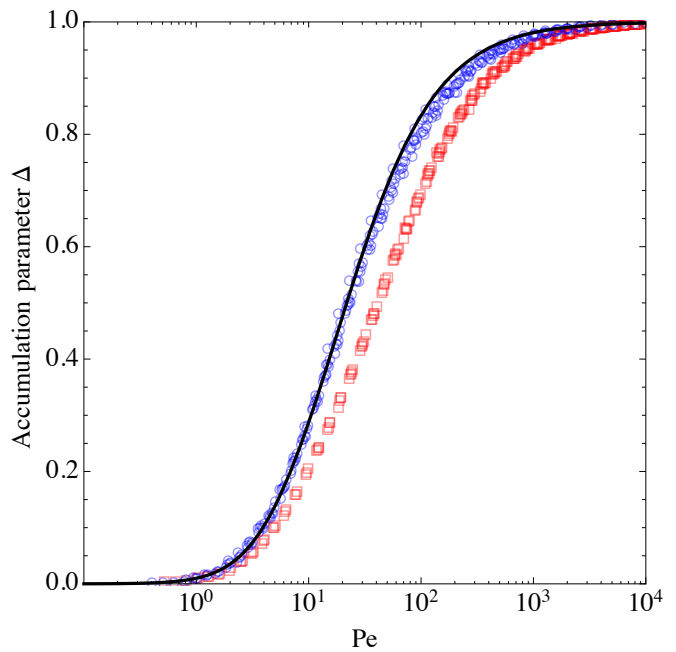


FIG. 2. Simulation results for a system of not interacting propelled colloidal particles with different Pe . The blue circles correspond to systems with $\ell_p/\ell \approx 1/32$, the red squares to systems with $\ell_p/\ell \approx 1/4$ (cf. Eq. (14)). The curve is the result Eq. (13) plugged into Eq. (8).

v_{sp} and persistence time $\tau_p = 2/D_r$ [34], where the mean square displacement is given by (cf. also [12])

$$\langle (\mathbf{r}(t) - \mathbf{r}(0))^2 \rangle = 4Dt + \frac{(v_{sp}\tau_p)^2}{2} \left(\frac{2t}{\tau_p} + e^{-\frac{2t}{\tau_p}} - 1 \right). \quad (11)$$

This includes the known limits of ballistic motion at short time scales and diffusive motion with an effective diffusion constant at long time scales. Thus, we get in the active region \mathcal{A} the effective diffusion constant

$$D_{\mathcal{A}} = D + \frac{\tau_p v_{sp}^2}{4} = D \left(1 + \frac{Pe^2}{6} \right) \quad (12)$$

leading to

$$\alpha = \sqrt{1 + \frac{Pe^2}{6}} - 1. \quad (13)$$

To confirm this result we performed several computer simulations of a two-dimensional system of 100 non-interacting mono-sized particles in a simulation cell with a region \mathcal{P} of $\phi = \pi/25$. The stochastic equations of motion have been solved using Euler's method.

In Fig. 2 we observe agreement between the theoretical estimate and results of computer simulations. However, the theory with solely diffusion coefficients works well on length scales large compared to the persistence length ℓ_p . The introduction of a finite length by virtue of the

width ℓ of \mathcal{A} can become important when ℓ is not large compared to the persistence length

$$\ell_p = 2\sqrt{D_{\text{eff}}\tau_p}. \quad (14)$$

The reason is that the drop of the density between the passive and the active region from ρ_p to ρ_A is not sharp, but takes place on the length scale ℓ_p in the active region: In the active region a boundary layer is created which scales with ℓ_p . No matter where the boundary layer is formed, any contribution of swimmers to the boundary layer reduces accumulation. This effect is negligibly small for huge system sizes ($\ell \gg \ell_p$), but leads to a severe drop of Δ in the other limit, where the density ρ_A as defined in Eq. (10) is no longer reached.

The here described accumulation in passive regions is related to the athermal phase separation of interacting particles [19–22], where the collision of particles leads to a reduced effective diffusion coefficient depending on the particle density, which again results in the emergent creation of clusters above a certain packing fraction (cf. below). However, the here described phenomenon occurs at any density and the region of accumulation is controlled; any spontaneously created clusters form and dissolve dynamically. The interplay between self-clustering and trapping is discussed in the next paragraph.

B. Increased particle density

While in the preceding section the interaction between particles was neglected, we now consider particles with a hard core repulsion as introduced in Eq. (2). The interaction introduces – additionally to the persistence length – a second length-scale given by the mean particle distance which depends on the particle density. Because we use a strong repulsion ($\epsilon = 100k_B T$) and the mean particle distance in closed packed system depends on the particle density, we choose as a length scale the truncation length $2^{1/6}\sigma$, and define a particle volume fraction

$$\phi_p = \frac{N\pi\sigma^2 2^{1/3}}{V}. \quad (15)$$

Analogous, we may define a volume fraction in the passive region, $\phi_{p,\mathcal{P}}$, and one in the active region $\phi_{p,\mathcal{A}}$.

We may now deduce a maximal accumulation of particles using the finite *capacity* of the passive region – once the passive region is filled, no more active particles can enter. At least when the local volume fraction in the passive region exceeds the hexagonal closed packing value with lattice constant $2^{1/6}\sigma$, the accumulation is *reduced* compared to the noninteracting case. This is the case for particle volume fractions exceeding

$$\phi_p^{\text{max}} = \phi \frac{\pi}{2\sqrt{3}}. \quad (16)$$

In Fig. 3 we observe the reduction of accumulation for $\phi_p > \phi_p^{\text{max}}$. Using the hexagonal closed packing particle

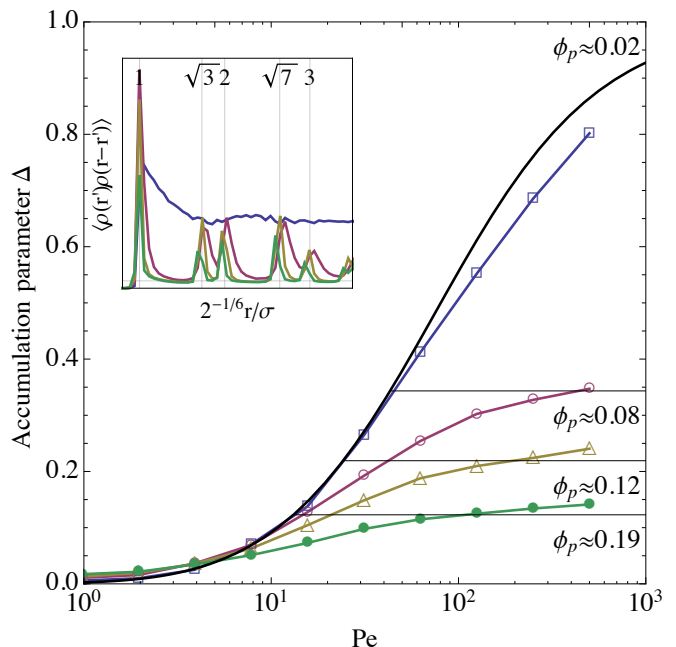


FIG. 3. Accumulation for interacting active colloidal particles with volume fractions ϕ_p and a passive region of relative size $\phi = \pi/100$. The horizontal lines represent accumulation parameters for the case $\phi_{p,\mathcal{P}} = \pi/(2\sqrt{3})$ with lattice constant $2^{1/6}\sigma$, which is only an upper estimate, as higher densities produce smaller lattice constants. Interaction effects are expected for densities exceeding $\phi_p^{\text{max}} \approx 0.028$, where passivated particles align in a hexagonal lattice. In the inset the pair correlation function for $Pe = 250$ is shown. The shift of the peaks to reduced distances with increasing densities represents a reduction of the lattice constant.

density in the passive region (cf. Fig. 1) gives a good estimate for the accumulation parameter in the high-Pe limit,

$$\Delta_{\text{max}}(\phi_p, \phi) = \frac{\phi}{1 - \phi} \left(1 - \frac{\pi}{2\sqrt{3}\phi_p} \right). \quad (17)$$

For high particle densities, smaller lattice constants compared to the truncation length, leading to an increased accumulation compared to our estimate.

C. High particle density: Dynamic clustering

Above, we focussed on an accumulation in the passive region. But how is the interplay between this diffusion-stimulated accumulation discussed so far and spontaneous clustering which finally leads to the athermal phase separation e.g. observed at $\phi_p \gtrsim 0.4$ in Ref. [19]? Therefore, we first recapitulate the responsible mechanism for the latter: Active particles which collide can get stuck and create a cluster, if they are oriented towards each other. We define a cluster as a composition of at least three particles, with distances less than $2^{1/6}\sigma$. A dynam-

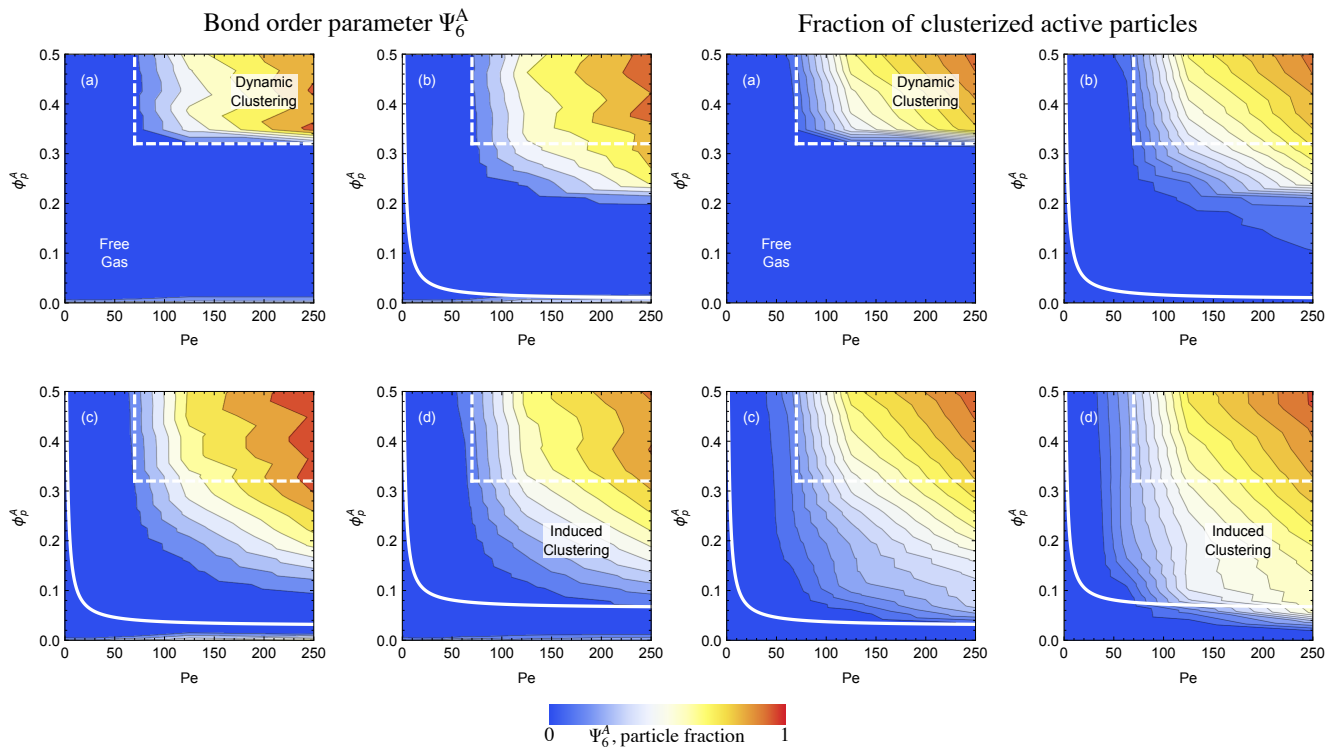


FIG. 4. Phase diagram depending on activity and density of active particles in the active region, expressed by the *active* bond order parameter as well as the clustered fraction of particles for (a) $\phi = 0$ (no passive region) and (b-d) $\phi = \pi/400, \pi/100, 9\pi/400$. The white dashed square serves as a guide to the eye. The white curve indicates at which filling fraction the passive region is filled assuming a lattice constant $2^{1/6}\sigma$.

ically created cluster survives until a member of the cluster changes its orientation through orientational Brownian motion and evades, which takes some time τ_p . If within this time new particles have condensed at the cluster surface, inner particles remain until the outer ones reorient, leading to the emergent accumulation of one big cluster. This happens in the phase separated case for active particles at high activities and high densities, and is indicated in Fig. 4 (a) by an increased bond-order parameter which reads for a hexagonal lattice [35, 36]

$$\Psi_6 = \frac{1}{N} \left| \sum_i \psi_6(i) \right| \quad \text{with} \quad \psi_6(i) = \frac{1}{6} \sum_j e^{i6\theta_{ij}}, \quad (18)$$

with θ_{ij} being the bond angle between particle i and j and an arbitrary reference axis. If particle i is surrounded by six nearest neighbors in a hexagonal manner, the local order parameter $|\psi_6(i)|$ is 1. Ψ_6^A denotes the global order parameter for the active region only. Accordingly in Fig. 1, we observe many passivated particles with $|\psi_6(i)|=1$.

If a passive region is introduced, the clustering effect in the active region is influenced by a reduction of the particle density due to partial capturing of particles in the passive region. We account for this effect by calculating quantities with respect to the particle volume fraction in the active region only. Furthermore, we observe in

Fig. 1 that the diffusion-induced cluster grows beyond the boundary of the passive region, leading to cluster formation also in the active region at particle densities where the athermal phase separation in a purely active system does not take place. This effect is related to the athermal phase separation as well as the accumulation of active particles [13] or bacteria near walls [37]: Active particles impinging at the surface of the passively induced cluster first have to reorient, which takes some persistence time τ_p . As the collision partner of an impinging particle cannot evade (because it is stuck in the passive region), the rest time of an impinging particle is longer compared to that in a dynamically induced cluster. Thus, the passive region acts as a nucleation core for dynamic clustering, which can now take place at reduced densities.

In Figs. 4(b-d) we can observe a reduction of the minimal clustering density depending on the size of the passive region. Not shown here is a pinning effect: While in a purely active system the clusters diffuse freely, a passive region introduces a pinning site for the cluster. This makes the introduction of a passive region, in combination with the dynamic clustering, interesting for applications which require control of a target region of active particles.

V. CONCLUSION AND OUTLOOK

In this work a method to trap propelled colloidal particles is presented. It is based on the suppression of the propulsion mechanism, e.g., the introduction of a shading mask in a system of phoretically propelled particles. An accumulation parameter is defined on the basis of inhomogeneous diffusion for diluted systems, and confirmed by computer simulations. A finite size effect is pointed out, which explains why the defined parameter is only valid as an upper limit. For the case of increased particle densities, the impact of steric interactions between the active particles has been addressed, which leads to a decrease of the accumulation as soon as crystallization in the passive region occurs. A further increase of the particle density leads to the regime where dynamic cluster formation sets in. We observe an enhancement of the effect of athermal phase separation by the introduction of a passive region. The combination of trapping by passivation with dynamic clustering makes the emergent clusters more controllable: Targets can be marked by introducing an inhomogeneity into the system. The collective behavior of the active particles then leads to a strong concentration of active particles in the *target region*, which may fulfill their task. When the mark is removed again, the active particles can again disperse in the medium.

An important next step is the experimental verification of the results presented here. Concerning the case of dense systems, experiments already exist: In a system of *Escherichia Coli* bacteria [38] the system cell has been manipulated such that bacteria move with a different speed in different regions of the system, leading

to their accumulation in the region with lower velocity. In another experiment, the inverse effect has been observed in a system of SiO₂-Ag Janus particles in a H₂O₂ solution [39]: Irradiation with UV-light causes a photolysis reaction between Ag and H₂O₂ and finally results in a self-diffusiophoretic motion of the particles. The fuel-gradient causes a diminishing particle concentration towards the center of the UV spot. This effect even dominates phototaxis of the particles, which otherwise would generate an accumulation of particles in the spot.

Besides experimental comparison several other questions remain. The perhaps most important one is that of the impact of interactions between the particles. Hydrodynamic interactions between active particles have been neglected so far. However, it is known that hydrodynamic interactions can strongly influence the collective behavior of active colloids. In [40] for example, the existence of a harmonic trap in a system of active particles leads to the formation of a pump or a rectifier, as the hydrodynamic interaction leads to a parallel alignment of particles approximating particles. A similar effect can be expected for a system of active particles in an inhomogeneous medium.

ACKNOWLEDGMENTS

M.M. thanks C. Bechinger and F. Kümmel for stimulating discussions on dynamical clustering and particles in patterned media, which led to the study of higher densities of active particles. The authors thank Dietrich E. Wolf for discussions. A grant by the University of Duisburg-Essen for the promotion of young scientists is acknowledged.

-
- [1] P. Hänggi, Reviews of Modern Physics **81**, 387 (2009).
 - [2] P. Romanczuk, M. Bär, W. Ebeling, B. Lindner, and L. Schimansky-Geier, Eur. Phys. J. Special Topics **202**, 1 (2012).
 - [3] R. Dreyfus, J. Baudry, M. L. Roper, M. Fermigier, H. A. Stone, and J. Bibette, Nature **437**, 862 (2005).
 - [4] C. Mavroidis, A. Dubey, and M. L. Yarmush, Annu. Rev. Biomed. Eng. **6**, 363 (2004).
 - [5] J. Anderson, Annu. Rev. Fluid Mech. **21**, 61 (1989).
 - [6] R. Piazza and A. Parola, J. Phys. Condens. Mat. **20**, 153102 (2008).
 - [7] F. Jülicher and J. Prost, Eur. Phys. J. E **29**, 27 (2009).
 - [8] H.-R. Jiang, N. Yoshinaga, and M. Sano, Phys. Rev. Lett. **105**, 268302 (2010).
 - [9] L. Baraban, R. Streubel, D. Makarov, L. Han, D. Karausenko, O. G. Schmidt, and G. Cuniberti, ACS Nano **7**, 1360 (2013).
 - [10] R. Golestanian, T. Liverpool, and A. Ajdari, Phys. Rev. Lett. **94**, 220801 (2005).
 - [11] R. Golestanian, T. B. Liverpool, and A. Ajdari, New J. Phys. **9**, 126 (2007).
 - [12] J. Howse, R. Jones, A. Ryan, T. Gough, R. Vafabakhsh, and R. Golestanian, Phys. Rev. Lett. **99**, 048102 (2007).
 - [13] G. Volpe, I. Buttinoni, D. Vogt, H.-J. Kümmerer, and C. Bechinger, Soft Matter **7**, 8810 (2011).
 - [14] I. Buttinoni, G. Volpe, F. Kümmel, G. Volpe, and C. Bechinger, J. Phys. Condens. Mat. **24**, 284129 (2012).
 - [15] A. Kaiser, H. H. Wensink, and H. Löwen, Phys. Rev. Lett. **108**, 268307 (2012).
 - [16] M. Mijalkov and G. Volpe, Soft Matter **9**, 6376 (2013).
 - [17] M. Braun and F. Cichos, ACS Nano **7**, 11200 (2013).
 - [18] B. Qian, D. Montiel, A. Bregulla, F. Cichos, and H. Yang, Chem. Sci. **4**, 1420 (2013).
 - [19] Y. Fily and M. C. Marchetti, Phys. Rev. Lett. **108**, 235702 (2012).
 - [20] G. S. Redner, M. F. Hagan, and A. Baskaran, Phys. Rev. Lett. **110**, 055701 (2013).
 - [21] G. S. Redner, A. Baskaran, and M. F. Hagan, Phys. Rev. E **88**, 012305 (2013), 1303.3195.
 - [22] I. Buttinoni, J. Bialké, F. Kümmel, H. Löwen, C. Bechinger, and T. Speck, Phys. Rev. Lett. **110**, 238301 (2013).
 - [23] J. Stenhammar, D. Marenduzzo, R. J. Allen, and M. E. Cates, Soft Matter **10**, 1489 (2014).
 - [24] M. J. Schnitzer, S. M. Block, H. C. Berg, and E. M. Purcell, Symp. Soc. Gen. Microbiol. **46**, 15 (1990).

- [25] M. Schnitzer, Phys. Rev. E **48**, 2553 (1993).
- [26] M. E. Cates, Rep. Prog. Phys. **75**, 042601 (2012).
- [27] F. Kümmer and C. Bechinger, private communication.
- [28] E. M. Purcell, Am. J. Phys. **45**, 3 (1977).
- [29] H. C. Berg, *Random walks in biology* (Princeton University Press, 1993).
- [30] G. Uhlenbeck and L. Ornstein, Phys. Rev. **36**, 823 (1930).
- [31] A. Einstein, Annalen der Physik **19**, 371 (1906).
- [32] J. D. Weeks, D. Chandler, and H. C. Andersen, J. Chem. Phys. **54**, 5237 (1971).
- [33] Note that Stokes' friction coefficient γ exists strictly only in three dimensions. Actually, calculating the friction coefficient of a disk moving in two dimensions would lead to the Stokes paradoxon [41, 42].
- [34] Sometimes in literature, the persistence time is introduced using $1/D_r$. However, a derivation from the Langevin equation (e.g. conducted in Ref. [43]) leads to the transition from ballistic to diffusive behavior in Eq. (11) at $2/D_r$, which makes this definition of τ_p more reasonable.
- [35] D. Nelson and B. Halperin, Phys. Rev. B **19**, 2457 (1979).
- [36] H. Schmidle, C. K. Hall, O. D. Velev, and S. H. L. Klapp, Soft Matter **8**, 1521 (2012).
- [37] D. Takagi, J. Palacci, A. B. Braunschweig, M. J. Shelley, and J. Zhang, Soft Matter **10**, 1784 (2014).
- [38] M. Demir and H. Salman, Biophys. J. **103**, 1683 (2012).
- [39] A. Sen, M. Ibele, Y. Hong, and D. Velegol, Farad. Discuss. **143**, 15 (2009).
- [40] M. Hennes, K. Wolff, and H. Stark, Phys. Rev. Lett. **112**, 238104 (2014).
- [41] G. G. Stokes, Cambridge Philosophical Society Transactions **9**, 259 (1851).
- [42] H. Lamb, *Hydrodynamics*, sixth edit ed., Dover Books on Physics (Dover publications, New York, 1932).
- [43] B. ten Hagen, S. van Teeffelen, and H. Löwen, J. Phys. Condens. Mat. **23**, 194119 (2011).